



Cite this: *Org. Biomol. Chem.*, 2025, **23**, 7521

Received 14th May 2025,  
Accepted 21st July 2025

DOI: 10.1039/d5ob00800j

rscl.li/obc

## Thiourea and squaramide organocatalysts for the asymmetric total synthesis of natural compounds

Márcia Rénio and M. Rita Ventura \*

Thiourea and squaramide organocatalysts have become essential tools in asymmetric synthesis, offering metal-free, highly selective methods for the efficient synthesis of complex natural products with important biological activities. Through directional hydrogen bonding, these catalysts activate electrophilic substrates with remarkable stereocontrol. This short review highlights recent advances demonstrating the power of these catalysts in the enantioselective synthesis of intricate natural scaffolds.

### Introduction

Organocatalysis has emerged over the past two decades as a powerful and versatile approach in synthetic organic chemistry, offering an alternative to traditional metal-based catalysis.<sup>1</sup> The appeal of organocatalysts lies in their operational simplicity, low toxicity, environmental friendliness and the ability to promote highly stereoselective reactions. Moreover, the compatibility of organocatalysts with a wide range of functional groups and their efficacy under mild conditions have contributed to the development of novel synthetic method-

ologies, including asymmetric transformations, cascade reactions and organocatalytic polymerisations.<sup>2,3</sup>

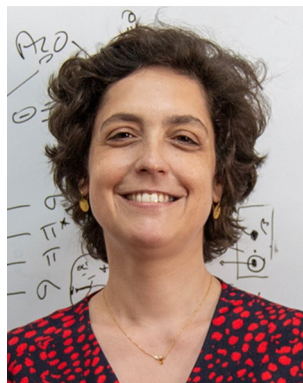
Thiourea-based organocatalysts have played a pivotal role in the evolution of non-metal catalysis, establishing themselves as a powerful class of hydrogen-bonding catalysts in organic synthesis. The concept of using thioureas as organocatalysts goes back to early studies on molecular recognition and anion binding in the 1990s.<sup>4–8</sup> However, it was not until the groundbreaking work of Schreiner<sup>9,10</sup> and Jacobsen<sup>11–14</sup> that the catalytic potential of thioureas was first demonstrated in the promotion of a wide range of synthetically valuable transformations. Thiourea organocatalysts work primarily through non-covalent dual hydrogen-bonding interactions, enabling the activation of a wide range of electrophilic substrates.<sup>11,14,15</sup> The central mode of activation involves the bifunctional hydro-

*Instituto de Tecnologia Química e Biológica António Xavier, Universidade Nova de Lisboa, Av. da República, 2780-157 Oeiras, Portugal. E-mail: rventura@itqb.unl.pt*



**Márcia Rénio**

*Márcia Rénio received her MSc in Chemistry from Universidade de Coimbra. Following this, she joined the Bioorganic Chemistry group at ITQB NOVA, where she completed her PhD in 2023. Her doctoral research, titled “Development of New Thiourea Organocatalysts for Asymmetric Reactions”, focused on the design and synthesis of thiourea-based organocatalysts derived from naturally occurring chiral scaffolds, specifically tartaric and camphoric acids. These catalysts were applied in various asymmetric transformations, including Michael additions and glycosylation reactions, demonstrating their versatility and potential in stereoselective organic synthesis.*



**M. Rita Ventura**

*Maria Rita Ventura has been the head of the Bioorganic Chemistry Laboratory at ITQB NOVA since October 2005. She studied Pharmaceutical Sciences at Faculdade de Farmácia, Universidade de Lisboa (1995) followed by doctoral studies in Organic Synthesis at Instituto de Tecnologia Química e Biológica António Xavier, Universidade Nova de Lisboa (1999). Her main research interests are asymmetric synthesis, stereoselective organocatalysis, biocatalysis, carbohydrate chemistry, the total synthesis of natural compounds and analogues with improved biological properties and medicinal chemistry.*



gen-bond donation from the N–H groups of the thiourea moiety to electron-deficient functional groups such as carbonyls, imines, nitroalkenes and activated esters. This interaction stabilises the developing negative charge in the transition state and lowers the LUMO energy of the electrophile, thereby enhancing its susceptibility to nucleophilic attack. Chiral thiourea organocatalysts promote highly enantioselective reactions through precise organisation of the transition state.

In some organocatalysts, thiourea units are combined with basic or nucleophilic groups (amines or phosphines), enabling bifunctional catalysis.<sup>16–19</sup> In these cases, the thiourea activates the electrophile *via* hydrogen bonding, while the basic site activates the nucleophile, leading to enhanced reactivity and selectivity through concerted substrate activation.<sup>20–25</sup>

Several recent reviews have already been dedicated to the extraordinary role of thiourea-based catalysts in stereoselective reactions and enantioselective total synthesis.<sup>26–38</sup>

Squaramide-based organocatalysts have gained increasing prominence in asymmetric catalysis due to their superior hydrogen-bond-donating ability, structural rigidity and tunable electronic properties. In many cases, squaramide analogues exhibit higher catalytic activity and selectivity, attributed to stronger and more directional hydrogen-bond interactions due to the increased acidity of the N–H groups, when compared with thiourea-based catalysts. The cyclic squaramide, being rigid planar, provides a highly organised geometry, which facilitates higher stereochemical control.

The synthesis of natural products with complex and densely functionalised architectures remains a central challenge in organic chemistry. Thiourea and squaramide organocatalysts have emerged as powerful tools in addressing this challenge, owing to their ability to activate electrophilic substrates through precise and directional hydrogen-bonding interactions. These organocatalysts are particularly effective in promoting highly selective asymmetric transformations under mild, metal-free conditions, making them well-suited for the construction of stereochemically rich natural products. Their bifunctional nature allows simultaneous activation of both nucleophilic and electrophilic partners, enabling efficient cascade reactions and stereoselective bond formations. As such, thiourea and squaramide catalyses have become indispensable strategies in the enantioselective total synthesis of alkaloids, terpenes and other bioactive natural scaffolds.

In this non-comprehensive review, we illustrate the usefulness of thiourea and squaramide organocatalysts for the elegant and efficient asymmetric synthesis of complex and very challenging natural compounds, with selected recent examples.

## Applications of thiourea and squaramide organocatalysts in asymmetric total syntheses

Aspidosperma alkaloids constitute a large and structurally diverse family of monoterpene indole alkaloids predomi-

nantly isolated from the *Aspidosperma* genus (family Apocynaceae). These alkaloids are characterised by a pentacyclic or tetracyclic core. The structural complexity of Aspidosperma alkaloids, which includes numerous stereocenters and challenging ring systems, makes them important targets in synthetic organic chemistry. Biologically, Aspidosperma alkaloids have attracted significant interest due to their diverse pharmacological properties, including antitumor, antimalarial, antihypertensive and CNS-modulating activities.<sup>39</sup> Members of this family of alkaloids have served as scaffolds for drug discovery and as synthetic intermediates for the synthesis of more complex natural products.

Tibor Soós and collaborators described the gram scale synthesis of (–)-minovincine **1** and (–)-aspidofractinine **2** in eight steps (Scheme 1).<sup>40</sup> These two compounds belong to the Aspidosperma alkaloid family,<sup>41</sup> monoterpene indole alkaloids which present a complex structure with several quaternary carbon stereocentres.

Due to its challenging structure, the enantioselective synthesis of (–)-minovincine **1** has previously only been described by David MacMillan in 2013,<sup>42</sup> and Atsushi Nishida in 2015.<sup>43</sup> The first enantioselective total synthesis of **1** by MacMillan and coworkers relied on an organocatalytic Diels–Alder/ $\beta$ -elimination/conjugate addition cascade, catalysed by a MacMillan imidazolidinone organocatalyst (iminium catalysis). The key asymmetric intermediate was obtained with 91% ee, 72% yield and (–)-minovincine was obtained in 9 steps from commercially available starting materials. Nishida's catalytic enantioselective total synthesis of (–)-minovincine involved an asymmetric Diels–Alder reaction catalysed by a chiral holmium catalyst. Their key intermediate was obtained with 94% ee.

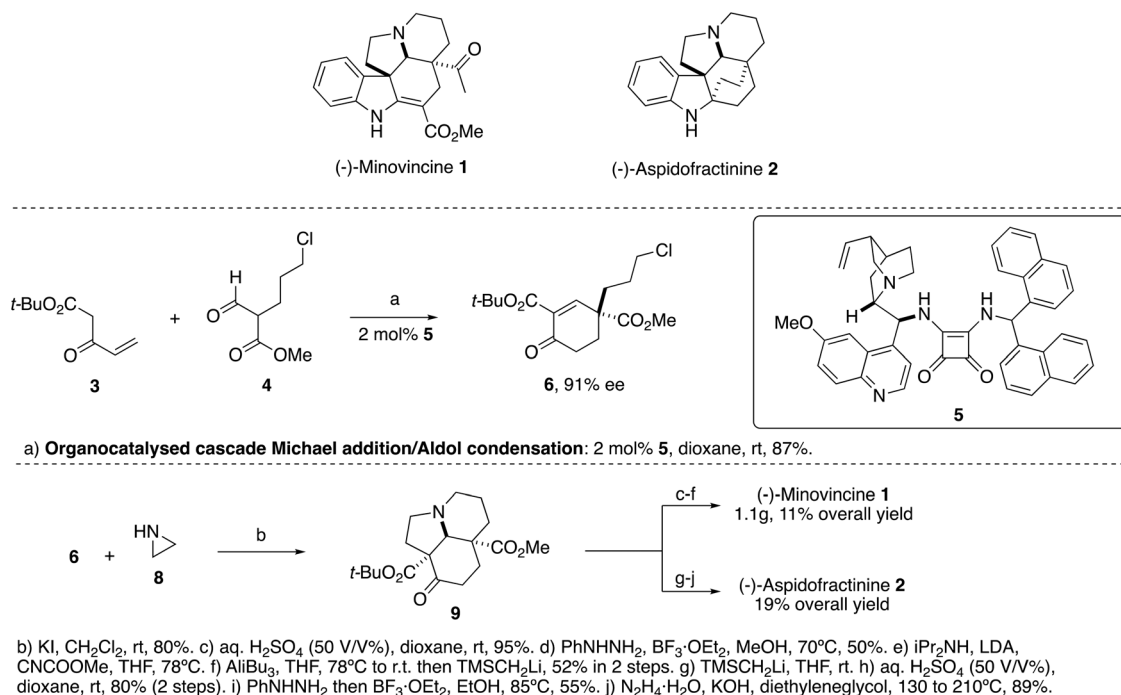
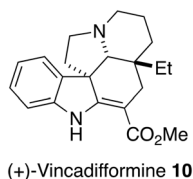
The strategy developed by Soós was based on an organocatalytic Michael addition/aldol condensation catalysed by the previously described quinine-squaramide organocatalyst **5** (Scheme 1).<sup>44</sup> This reaction was scaled up to 100 g, affording enone **6** in 87% yield and 91% ee.

The key tricyclic intermediate **9** was constructed from enone **6** *via* another cascade strategy involving a multistep anionic Michael/SN<sub>2</sub> cascade reaction in 72% yield on a 50 g scale (Scheme 1). From **9**, (–)-minovincine **1** and (–)-aspidofractinine **2** were synthesised, both requiring only 4 additional steps.<sup>40</sup> In summary, four contiguous stereogenic centres were generated with exceptional control over both absolute and relative stereochemistry. The strategic implementation of cascade transformations, coupled with sterically governed chemoselectivity and regioselectivity, was instrumental in achieving a concise synthetic route towards these challenging molecules.

(+)-Vincadifformine **10** is another member of the Aspidosperma alkaloid family (Fig. 1),<sup>45</sup> and its asymmetric total synthesis based on a thiourea organocatalysed strategy was described by Gang Zhao and co-workers.<sup>46</sup>

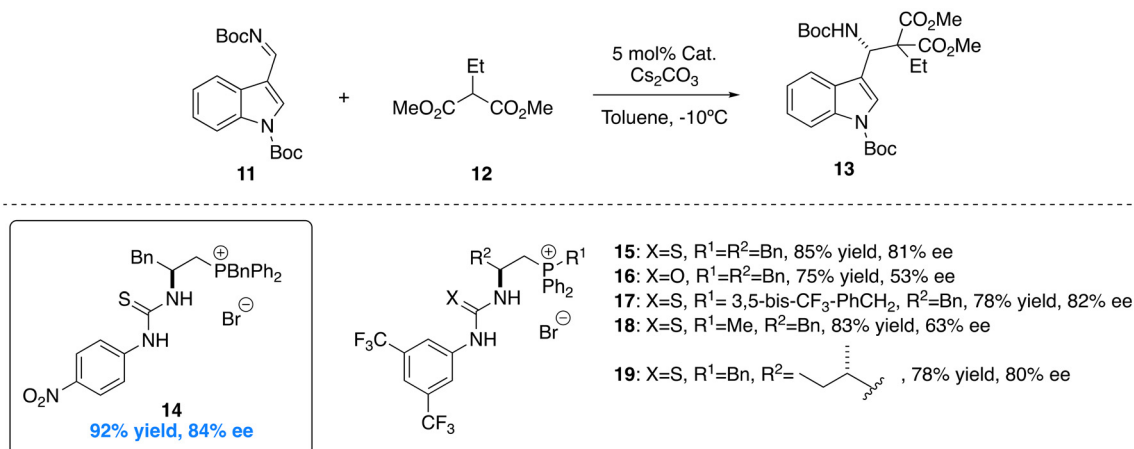
Vincadifformine and its analogues exhibit potent cytotoxic activity *in vitro* across a panel of 60 human tumor cell lines representing nine distinct cancer types.<sup>47</sup> Using an organocatalysed strategy, MacMillan previously described the synthesis of



Scheme 1 Synthesis of (-)-minovincine **1** and (-)-aspidofractinine **2**.Fig. 1 Structure of (+)-vincadifformine **10**.

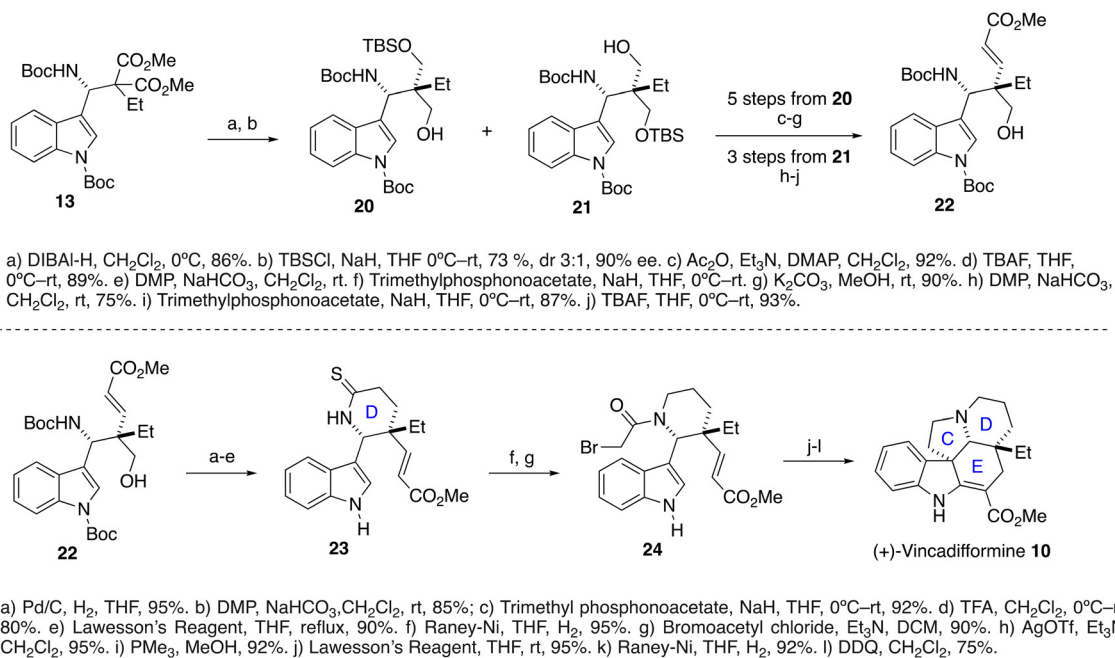
vincadifformine **10** and structurally core related alkaloids by means of organocascade catalysis involving a Diels–Alder/ $\beta$ -elimination/amine conjugate addition sequence catalysed by an imidazolidinone organocatalyst, affording 83% yield and excellent enantioselectivity (97% ee).<sup>48</sup>

Zhao and co-workers employed a chiral bifunctional thiourea-phosphonium salt to catalyse the asymmetric Mannich reaction between *N*-Boc indole aldimine **11** and dimethyl ethylmalonate **12** to afford **13** (Scheme 2). Organocatalyst **14** afforded the best results, 92% yield and 84% ee, from the six chiral thioureas screened (Scheme 2).



Scheme 2 Screening of chiral catalysts.





**Scheme 3** Synthesis of (+)-vincadifformine **10**.

From the key intermediate **13**, the synthesis of (+)-vincadifformine **10** was achieved (Scheme 3), with high stereocontrol in the construction of the additional two asymmetric carbons.

The efficient construction of the D ring was achieved through a TFA-promoted deprotection/amidation cascade process, affording intermediate **23** in 5 steps. The absolute configuration of **23** was confirmed by X-ray analysis. Construction of the C ring was achieved by an intramolecular alkylation, previously described by Heathcock and Toczko for the synthesis of aspidospermidine.<sup>49</sup> Finally, a phosphine-promoted aza-Morita–Baylis–Hillman reaction was the key reaction for the construction of the E ring (Scheme 3).

Very recently, Alakesh Bisai and co-workers reported the total synthesis of (–)-calycanthine **25**, (+)-chimonanthine **26** and (+)-folicanthine **27** (Fig. 2).<sup>50</sup>

Calycanthaceae alkaloids are a distinctive class of indole-based natural products predominantly isolated from plants of the Calycanthaceae family, including genera such as

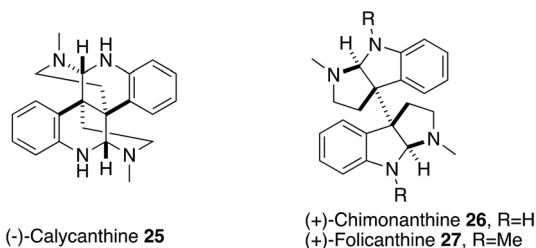


**Fig. 2** Structures of (–)-calycanthine **25**, (+)-chimonanthine **26** and (+)-folicanthine **27**, members of the Calycanthaceae alkaloid family.

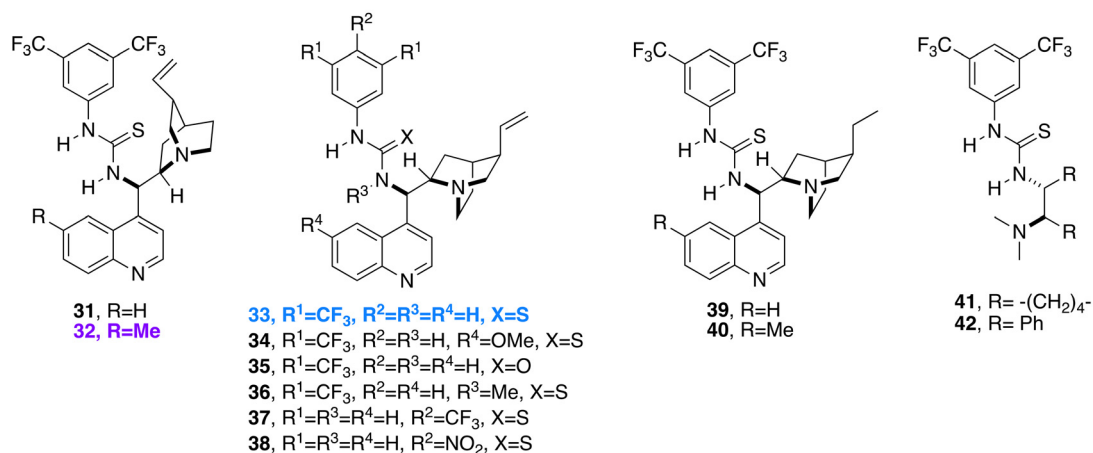
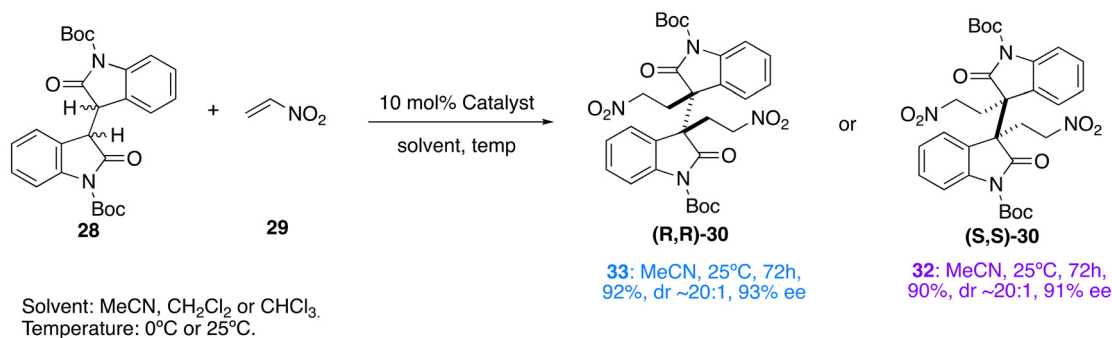
*Calycanthus* and *Chimonanthus*.<sup>51</sup> These alkaloids are characterised by complex polycyclic structures and are biosynthetically derived from tryptamine and related amino acid precursors through oxidative dimerisation pathways.<sup>52</sup> The intricate architectures of these alkaloids have posed substantial challenges for synthetic chemists, prompting the development of various strategies to achieve their total synthesis.<sup>46,53–57</sup>

Pharmacologically, Calycanthaceae alkaloids have demonstrated a broad spectrum of biological activities. Notably, they exhibit anti-convulsant, anti-fungal, anti-viral, analgesic, anti-tumour and melanogenesis inhibitory properties. These bioactivities have spurred interest in their potential therapeutic applications and have driven further research into their mechanisms of action.<sup>58</sup>

The synthetic strategy developed by Bisai and co-workers was based on a thiourea catalysed sequential Michael addition of bis-oxindole **28** to nitroethylene **29** (Scheme 4). Several differently amine protected dimeric 2-oxindoles were screened; however, the best results (enantioselectivity, diastereoselectivity and yield) were obtained with *N*-Boc protected **28**. Acetonitrile and dichloromethane were evaluated as solvents, with acetonitrile affording the best results. Interestingly, using different thiourea selected catalysts, each enantiomer of **30** was obtained in high yield, enantioselectivity and diastereoselectivity (Scheme 4). The authors proposed a mechanism of action for this Michael addition.<sup>50</sup>

From (*R,R*)-**30**, the asymmetric syntheses of (–)-calycanthine **25**, (+)-chimonanthine **26** and (+)-folicanthine **27** were completed, 6 steps/41% yield, 5 steps/68% yield and 6 steps/56% yield, respectively. From the enantiomer (*S,S*)-**30**, the corresponding enantiomers of these three compounds were also successfully synthesised, as expected.





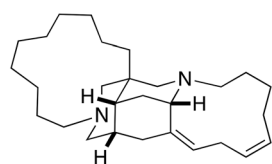
**Scheme 4** Catalyst screening for the sequential Michael addition of bis-oxindole **28** to nitroethylene **29**.

The 30-step total synthesis of madangamine E **43**, a complex marine alkaloid with notable biological activity, was recently described by Darren Dixon and Trevor Hamlin.<sup>68</sup>

Madangamine E **43** (Fig. 3) is part of a family of polycyclic alkaloids, the madangamine family isolated from marine sea sponges belonging to the genus *Xestospongia*.<sup>59–61</sup> Madangamines have been known for their cytotoxic and anti-proliferative properties, making them valuable targets in medicinal chemistry.<sup>62,63</sup> Their intricate structures, featuring a pentacyclic fused ring system with multiple stereocentres and macrocyclic rings, pose significant synthetic challenges.<sup>64–67</sup>

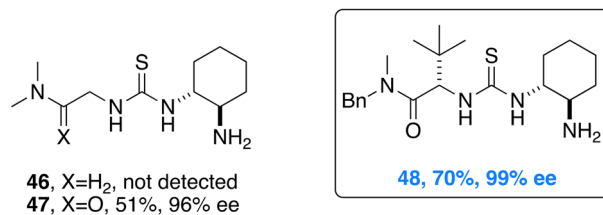
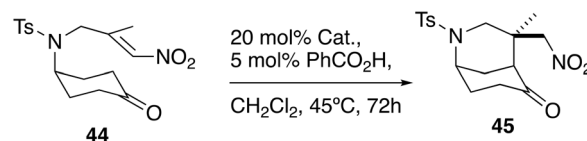
With the aim to synthesise enantiopure madangamine E **43**, Dixon and Hamlin and coworkers developed a highly enantioselective organocatalytic desymmetrisation reaction (Scheme 5).<sup>68</sup> The rigid bicyclic system was important to

induce high stereoselectivity in subsequent key steps for the synthesis of the target molecule **43**. This reaction involved an intramolecular Michael addition of a prochiral ketone to a tethered  $\beta,\beta'$ -disubstituted nitroolefin, catalysed by a primary amine–thiourea catalyst. The enantioselective desymmetrisation Michael reaction was first optimised by screening eleven organocatalysts using the 4-aminocyclohexanone **44**. From the eleven organocatalysts screened,<sup>68</sup> only **47** and **48** afforded the



Madangamine E **43**

**Fig. 3** Structure of madangamine E **43**.



**Scheme 5** Catalyst screening for the desymmetrisation intramolecular Michael addition of nitroolefin **44**.



cyclised product **45** (Scheme 5), the best one being Jacobsen's thiourea catalyst **48** (70% yield, 99% ee).

Density functional theory (DFT) calculations provided insight into the reaction's enantioselectivity, revealing that hydrogen bonding interactions between the catalyst and substrate played a crucial role in stabilising the transition state.

This highly efficient, enantioselective and diastereoselective organocatalytic desymmetrisation reaction was subsequently applied to the total synthesis of madangamine E. For this, nitroolefin **51** was synthesised in 9 steps starting from 1,4-cyclohexanedione monoethylene acetal **49** (Scheme 6), on a gram scale, affording the geometric isomers **51** and **52**.<sup>68</sup> The enantioselective desymmetrisation reaction catalysed by thiourea **48** using nitroolefin **51** as the starting material was successfully performed on a more than 5 g scale. This organocatalysed reaction efficiently constructed the chiral bicyclic core **53**, establishing three stereogenic centers, including a quaternary carbon, with near perfect enantio- and diastereoselectivity (>99% ee, only one diastereoisomer) and high yield (95%) on a multigram scale (Scheme 6).

Following the establishment of the bicyclic core, this elegant and remarkable total synthesis of madangamine E incorporated several strategic transformations including a one-pot oxidative lactamisation to form the B ring system; two-step Z-selective olefination of a sterically hindered ketone; and ring-closing metathesis (RCM) reactions to construct the macrocyclic rings D and E.

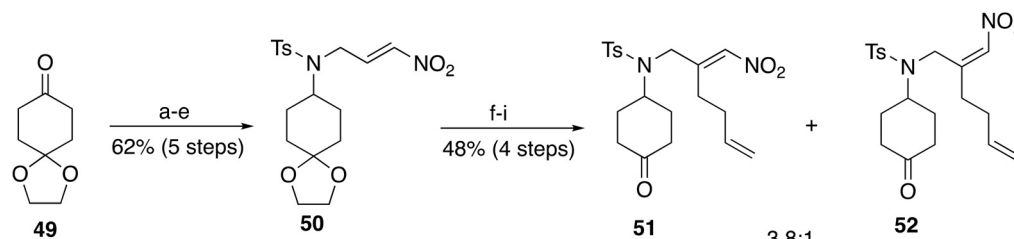
Thiourea organocatalysts were equally important for the synthesis of another highly complex natural product, capramazacyn A **54** (Fig. 4), described by Yoshiji Takemoto and his team.<sup>69</sup>

Caprazamycins were isolated from *Streptomyces* sp. MK730-62F2,<sup>70,71</sup> and they belong to a unique class of nucleo-

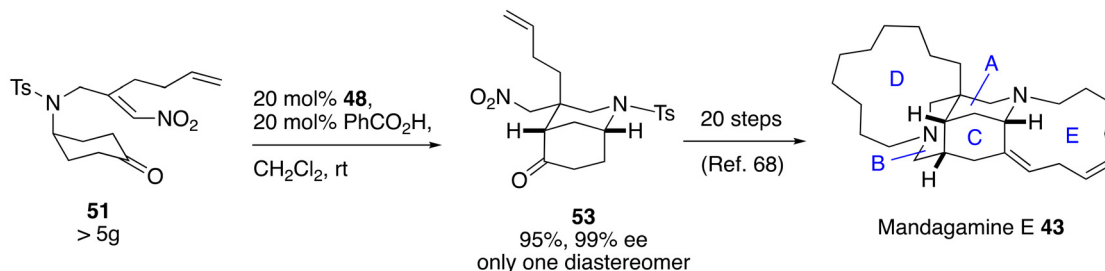
side antibiotics that inhibit bacterial cell wall biosynthesis, specifically targeting MraY, an essential membrane-associated enzyme involved in the early steps of peptidoglycan (cell wall) formation. This mechanism is distinct from traditional antibiotics like  $\beta$ -lactams and glycopeptides. These molecules possess an unusual and complex structure, with a liponucleoside core, 1,4-diazepanone ring and long fatty acid side chain. Caprazol **55** is the core structure of caprazamycins (Fig. 4).

Takemoto and co-workers reported a new synthesis that relied on a practical and scalable method to synthesise *syn*- $\beta$ -hydroxyamino acid derivatives. This was achieved through a diastereoselective aldol reaction of uridine-derived aldehydes with diethyl isocyanomalonate and phenylcarbamate, using thiourea catalysts or bases (Table 1).

Table 1 presents a summary of the best yields and diastereomeric ratios (dr) achieved under various reaction conditions. In entries 1 to 4, where aldehyde **56** was used in combination with organocatalyst (*S,S*)-**61**, varying the catalyst loading had a clear impact on both yield and stereoselectivity. At 10 mol% catalyst loading (entry 1), the reaction afforded 77% yield with a diastereomeric ratio of 6.5 : 1. When the catalyst loading was decreased to 7 mol% and 5 mol% (entries 2 and 3), the yield dropped slightly to 81% and 68%, respectively, accompanied by a gradual decline in diastereoselectivity to 5 : 1 and 4.2 : 1. The amount of organocatalyst also influenced the obtention of a byproduct (not represented).<sup>69</sup> This trend suggests that higher catalyst loadings favour both higher yields and better stereocontrol. Notably, switching the enantiomer of the catalyst to (*R,R*)-**61** (entry 4) reversed the stereochemical outcome dramatically, yielding a product with a diastereomeric ratio greater than 1 : 20, confirming the strong influence of catalyst chirality on the reaction selectivity.



a) Allylamine, NaBH(OAc)<sub>2</sub>, DCE. b) TsCl, Et<sub>3</sub>N, THF, 86% (2 steps). c) RuCl<sub>3</sub>, NaIO<sub>4</sub>, DCE, MeCN, H<sub>2</sub>O. d) MeNO<sub>2</sub>, Et<sub>3</sub>N, CH<sub>2</sub>Cl<sub>2</sub>, 80% (2 steps). e) MsCl, Et<sub>3</sub>N, CH<sub>2</sub>Cl<sub>2</sub>, 90%. f) But-3-en-1-ylmagnesium bromide, ZnCl<sub>2</sub>, CuCN, LiCl, THF, 90%. g) PhSeBr, *n*-BuLi, THF, 78%. h) H<sub>2</sub>O<sub>2</sub>, Et<sub>2</sub>O, CH<sub>2</sub>Cl<sub>2</sub>. i) 3M HCl, THF, 68% (2 steps).



Scheme 6 Synthesis of madangamine E **43**.



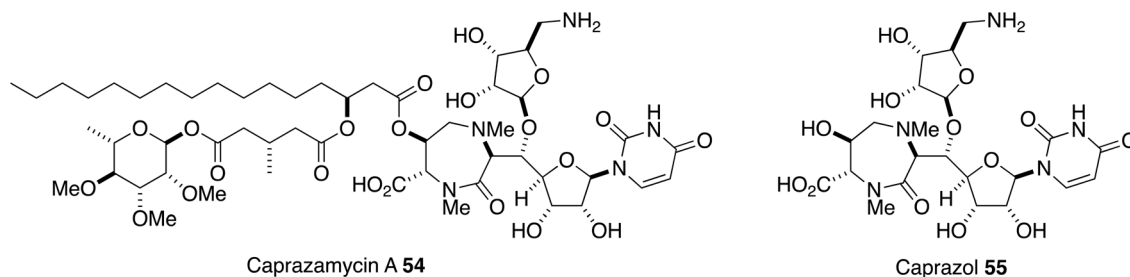


Fig. 4 Structures of caprazamycin A **54** and caprazol **55**.

Table 1 Optimisation of the diastereoselective aldol reaction of aldehydes **56**–**59** with thiourea catalysts or bases

Entry	Aldehyde	Nucleophile	Catalyst or base	Yield (%)	dr
1	<b>56</b>	<b>62</b>	( <i>S,S</i> )- <b>61</b> (10 mol%)	77	6.5 : 1
2	<b>56</b>	<b>62</b>	( <i>S,S</i> )- <b>61</b> (7 mol%)	81	5 : 1
3	<b>56</b>	<b>62</b>	( <i>S,S</i> )- <b>61</b> (5 mol%)	68	4.2 : 1
4	<b>56</b>	<b>62</b>	( <i>R,R</i> )- <b>61</b> (10 mol%)	80	>10 : 1
5	<b>57</b>	<b>62</b>	( <i>S,S</i> )- <b>60</b> (60 mol%) <sup>a</sup>	55	9 : 1
6	<b>57</b>	<b>62</b>	K <sub>2</sub> CO <sub>3</sub> (60 mol%) <sup>a</sup>	68	9 : 1
7	<b>58</b>	<b>62</b>	( <i>i</i> -Pr) <sub>2</sub> NET (10 mol%) <sup>b</sup>	71	13 : 1
8	<b>59</b>	<b>63</b>	K <sub>2</sub> CO <sub>3</sub> (100 mol%) <sup>b</sup>	84	>20 : 1

<sup>a</sup> 0 °C to rt. <sup>b</sup> 0 °C.

With aldehyde **57**, the use of organocatalyst (*S,S*)-**60** (entry 5) gave 55% yield and 9 : 1 dr, while switching to the inorganic base K<sub>2</sub>CO<sub>3</sub> (entry 6) improved the yield to 68% without compromising the diastereoselectivity, which remained at 9 : 1. This suggests that under certain conditions, a simple base can match the efficiency and selectivity of an organocatalyst. For aldehyde **58** (entry 7), the use of diisopropylethylamine as the base provided a good yield (71%) and high diastereoselectivity (13 : 1), indicating strong substrate-driven control over the reaction outcome. Finally, the best results were observed with aldehyde **59** (entry 8), where K<sub>2</sub>CO<sub>3</sub> as the base and nucleophile **63** afforded 84% yield and exceptional diastereoselectivity (>20 : 1). The thiourea catalyst enantiomer and loading critically influenced both the yield and stereochemical reaction outcome. Lower catalyst loadings tended to decrease both yield and dr. However, for certain substrates, base-mediated reactions could achieve comparable or even superior results compared to organocatalysis. The nature of the protecting group also played a significant role, with bulkier groups like TBS leading to higher diastereoselectivities. The authors performed

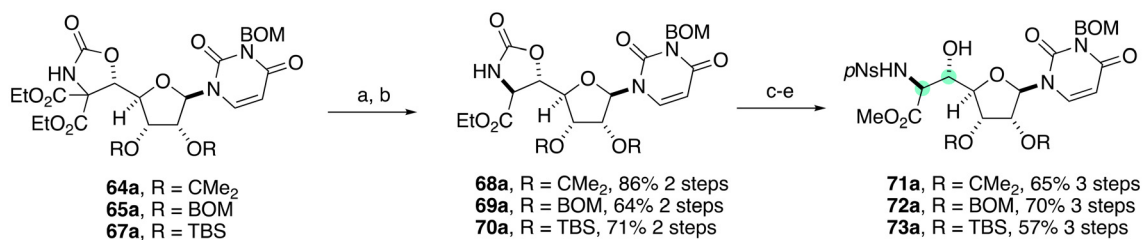
computational studies of the thiourea catalysed aldol reactions to rationalise the diastereoselectivity outcome of these reactions.

The synthesis of *syn*-β-hydroxyamino acid derivatives **71**, **72** and **73**, key intermediate compounds for the total synthesis of **54**, was accomplished from intermediates **64a**, **65a** and **67a**, in 5 steps (Scheme 7). The selective monohydrolysis of **64a**, **65a** and **67a** was followed by decarboxylation to afford the thermodynamically more stable *trans*-oxazolidinones **68**–**70**. Transesterification to the corresponding methyl esters was necessary for the oxazolidinone ring-opening. The *syn*-β-hydroxyamino acid derivatives **71**, **72** and **73** were obtained after amine protection with the *p*-nitrobenzenesulfonyl (*p*NS) group, followed by treatment with NaOMe in methanol for the ring opening (Scheme 7).

Compounds **71**–**73** were key intermediates for the synthesis of liponucleoside antibiotics.

The central 1,4-diazepanone ring, a distinctive feature of caprazol **55** and caprazamycin A **54**, was constructed starting from readily available L-(+)-diethyl tartrate in 15 or 16 synthetic





**Scheme 7** Synthesis of *syn*- $\beta$ -hydroxyamino acid derivatives **71a**, **72a** and **73a**. (a) KOH or LiOH, aq. THF. (b) DBU, THF, 70 °C. (c) Zn<sub>4</sub>(OCOCF<sub>3</sub>)<sub>6</sub>O, MeOH, 50 °C. (d) *p*NsCl, NaH, DMF. (e) NaOMe, MeOH.

steps, using a key Mitsunobu reaction, facilitating the formation of this challenging seven-membered ring. A stepwise sequence was employed to introduce the fatty acid side chain, a crucial component for the antibiotic's biological activity. A notable aspect of the synthesis was the global deprotection step, which utilised palladium black and formic acid. This method effectively removed protecting groups without hydrogenating the olefin present in the uridine moiety, completing the first total synthesis of caprazamycin A.<sup>69</sup> This comprehensive synthesis not only provides access to caprazamycin A for further biological studies but also offers a framework for the synthesis of related nucleoside antibiotics, potentially aiding in the development of new antimicrobial agents.

Tetracyclic indole alkaloids form an important class of natural compounds, known for their significant biological activities, with many being used as medicinal drugs.<sup>72</sup> As a result, tetracyclic indole alkaloids have attracted considerable synthetic interest, leading to numerous sophisticated total syntheses and several domino catalysis approaches.<sup>72–80</sup>

(+)-Peganumine A **74** (Fig. 5) is a natural dimeric tetrahydro- $\beta$ -carboline alkaloid, with a unique 3,9-diazatetracyclo-[6.5.2.0<sup>1,9</sup>.0<sup>3,8</sup>]pentadec-2-one scaffold, playing a significant role in biological applications.<sup>81</sup> Its important bioactivity and low isolation yield make the synthesis of (+)-peganumine A highly attractive.

Zhu and coworkers developed a seven-step, gram-scale, enantioselective total synthesis of (+)-peganumine A **74** in 33% overall yield, featuring three key steps: a Liebeskind–Srogl cross-coupling; a one-pot construction of the tetracyclic skeleton from an  $\omega$ -isocyano- $\gamma$ -oxoaldehyde *via* an unprecedented C–C bond-forming lactamisation followed by transannular condensation; and a one-pot organocatalytic process that merges two achiral building blocks into an octacyclic structure

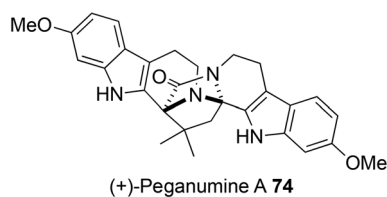


**Fig. 5** Structure of (+)-peganumine A **74**.

*via* an enantioselective Pictet–Spengler reaction, followed by transannular cyclisation.<sup>82</sup>

For the synthesis of building blocks **84** and **85**, a Liebeskind–Srogl cross-coupling reaction was necessary; this reaction proved to be challenging but after optimising the reaction parameters, the authors obtained the desired compounds **78** and **79** (4 step yield: 54% and 54% respectively, Scheme 8) followed by the obtention of the dehydration compounds **80** and **81** in 89% and 92% yields, respectively. The reaction of **80** or **81** with TFA in dichloromethane yielded tetracycle **82** or **83** (85% yield). Oxidation under Corey–Kim conditions afforded building blocks  $\alpha$ -ketolactam **84** and **85** (Scheme 8).<sup>83</sup>

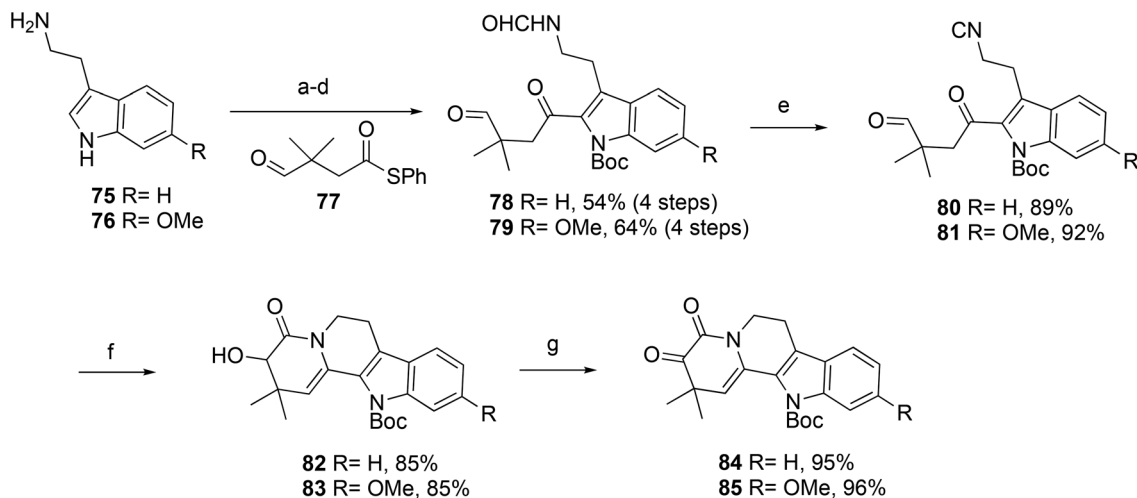
To obtain (+)-peganumine A **74**, the next step was the condensation of the synthesised compound **85** with 6-methoxytryptamine **86** (Scheme 9). For chiral induction, the authors chose to use chiral organocatalysts in the Pictet–Spengler reaction.<sup>83</sup> Chiral phosphoric acids are commonly used in this transformation;<sup>84–87</sup> however, when the authors applied this method, the target compound was obtained in a very low yield (7%) with poor enantioselectivity (er 64.5 : 35.5). To improve the outcome, Jacobsen's thiourea **87** was used as the catalyst,<sup>88–91</sup> and employing benzoic acid as the co-catalyst proved to be fundamental for the enantioselective outcome of the reaction.

After optimising the reaction conditions, (+)-peganumine A **74** was successfully obtained in 69% yield with high enantioselectivity (er 96 : 4) (Scheme 9). From intermediate **84**, using the same strategy, (+)-9'-demethoxy-peganumine A **88** was obtained in 67% yield and er 96 : 4. This remarkable organocatalysed reaction allowed the obtention of an octacyclic compound *via* a domino process involving first an enantioselective Pictet–Spengler reaction followed by a TFA catalysed transannular cyclisation, leading to the first asymmetric total synthesis of (+)-peganumine A **74**.<sup>83</sup>

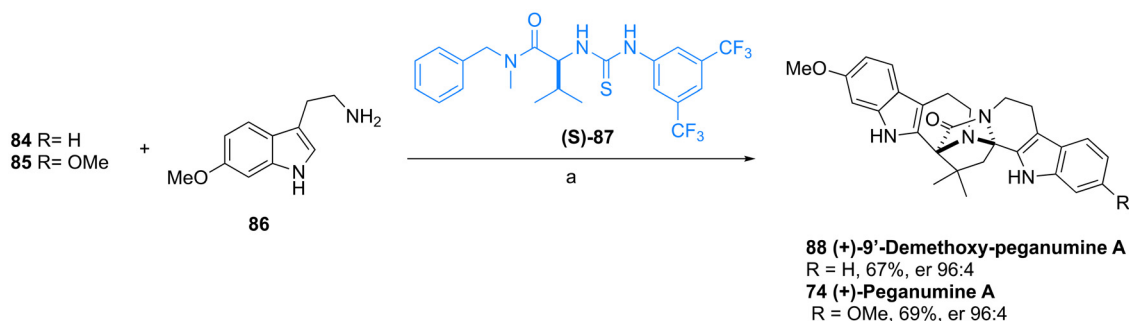
(+)-Arborisidine **89** is a natural pentacyclic monoterpene indole alkaloid with potential biological activities and extremely low natural abundance (Fig. 6). It was isolated from Malayan *K. arborea* Blume.<sup>92</sup> For this reason, several synthetic strategies have been developed, more specifically the total synthesis of (+)-arborisidine,<sup>93</sup> and several synthesis of related arboridinine **90**.<sup>94–96</sup>

Zhu's group established a five-step asymmetric synthesis for the preparation of (–)-arborisidine (–)-**89** (Scheme 10) fea-





**Scheme 8** Synthesis of tetracyclic  $\alpha$ -ketoamides **84** and **85**. (a) HCOOEt, 55 °C. (b) Boc<sub>2</sub>O, DMAP, DMF, rt. (c) i. TMPLi, THF, -78 °C and ii. Bu<sub>3</sub>SnCl. (d) **77**, Pd<sub>2</sub>dba<sub>3</sub>, CuDDP, AsPh<sub>3</sub>, hexane/THF 3/1, rt. (e) POCl<sub>3</sub>, Et<sub>3</sub>N, CH<sub>2</sub>Cl<sub>2</sub>, -78 °C. (f) TFA, Pyr, CH<sub>2</sub>Cl<sub>2</sub>, rt. (g) i. NCS, Me<sub>2</sub>S and ii. Et<sub>3</sub>N, CH<sub>2</sub>Cl<sub>2</sub>, -78 °C.



**Scheme 9** Synthesis of (+)-peganumine A **74** and (+)-9'-demethoxy-peganumine A **88**. (a) i. Toluene, 4 Å MS, reflux, 24 h, ii. (S)-**87** (0.2 equiv.), PhCOOH (0.2 equiv.), CH<sub>2</sub>Cl<sub>2</sub> (10% by volume), 35 °C, 4 days, and iii. TFA (0.2 equiv.), reflux, 2 days.

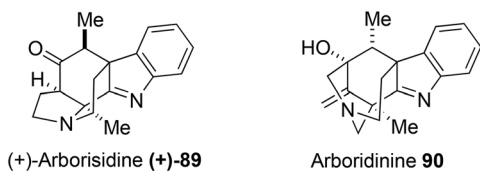


**Fig. 6** Structures of (+)-arborisidine (+)-**89** and arboridinine **90**.

turing three key steps: a regioselective Pictet–Spengler reaction, a chemo- and stereo-selective intramolecular oxidative cyclisation; and an aza-Cope/Mannich cascade followed by *in situ* oxidation and epimerisation.<sup>83</sup>

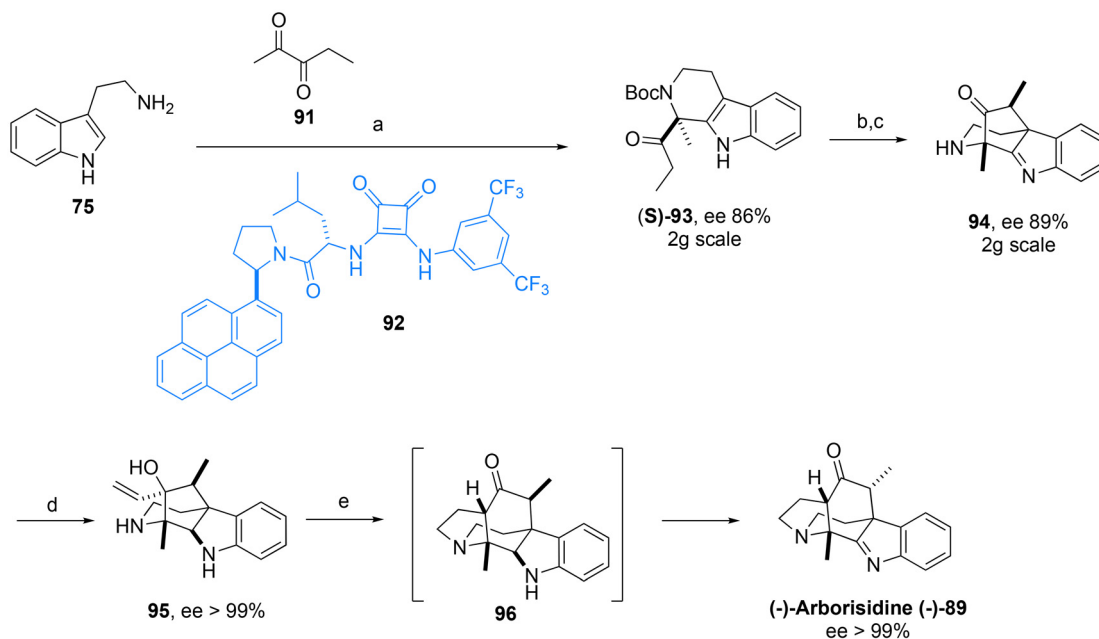
The first step was the enantioselective Pictet–Spengler reaction between tryptamine **75** and 2,3-pentanedione **91**. For this reaction, based on the authors' previous work<sup>83</sup> and the results obtained by Jacobsen,<sup>90,97</sup> several thio, urea and squaramide organocatalysts were evaluated. The screening showed that the

best organocatalyst for this transformation was the squaramide organocatalyst **92** (20 mol%), combined with *p*-nitrobenzoic acid (15 mol%) in toluene (0.04 M) at 5 °C for 12 days.

The next step involved protecting the amine with a Boc group, yielding (S)-**93**, in 53% yield, 86% ee, 2 g scale (Scheme 10). The subsequent intramolecular oxidative coupling of this compound, followed by reduction of the imine and removal of the amine-protecting group afforded **94**, also on a 2 g scale. The nucleophilic addition of vinylmagnesium bromide to the ketone in the presence of CeCl<sub>3</sub> afforded **95** in a 32% isolated yield with >99% ee. The starting material was recovered. The increase of the enantiopurity, from 88% ee to >99% ee, was hypothesised to be derived from the fact that the heterochiral magnesium or cerium amide complex of **94** was less soluble than the homochiral counterpart and therefore precipitated out of the reaction mixture. Interestingly, backing up this explanation the ee of the recovered **94** decreased from 89% to 84%.

The reaction of compound **95** with paraformaldehyde in degassed toluene/MeCN in the presence of TFA led to the for-





**Scheme 10** Synthesis of (-)-arborisidine (-)-89. (a) i. Organocatalyst **92** (20 mol%), *p*-nitrobenzoic acid (15 mol%), toluene (0.04 M), 5 °C, 12 days and ii.  $\text{Boc}_2\text{O}$ ,  $\text{Et}_3\text{N}$ , 53%. (b) LHMDS, PIDA, THF, -78 °C to rt, 58%. (c) i.  $\text{NaBH}_3\text{CN}$ , AcOH, MeOH, rt and ii. 4 N HCl, dioxane, 0 °C to rt, 73%. (d)  $\text{VinylMgBr}$ ,  $\text{CeCl}_3$ , THF, -78 °C, 32%. (e) i. TFA, paraformaldehyde, toluene/MeCN (3 : 1), rt, ii. PhIO, rt, and iii. 2 N aqueous KOH, rt, 61%.

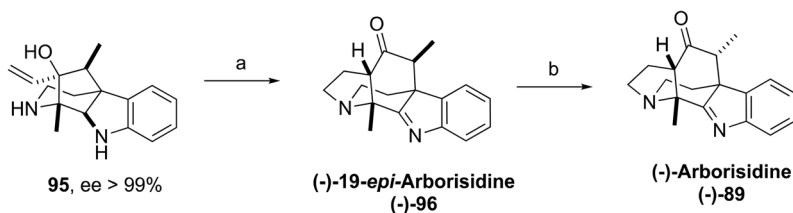
mation of pentacycle **96**, which was treated with iodobenzene followed by KOH treatment to afford (-)-arborisidine (-)-89 in 61% yield (Scheme 10). This compound is the enantiomer of the natural substance; however, the authors hypothesised that preparing the *ent*-catalyst **92** would likely enable the synthesis of (+)-arborisidine. The squaramide catalyst **92** was synthesised from *N*-Boc-pyrrolidine in 5 steps as described by Jacobsen.<sup>98</sup> (-)-Sparteine was used as a ligand to promote the enantioselective synthesis of an (*R*)-*N*-Boc-pyrenylpyrrolidine intermediate, which underwent peptide coupling with (*S*)-*N*-Boc-Leu to introduce the second asymmetric centre of the catalyst. Since both (+)-sparteine and (*R*)-Leu are commercially available, *ent*-Cat **92** could eventually be prepared and used to synthesise natural (+)-arborisidine.

Zhu and collaborators observed that when the entire aza-Cope/Mannich/oxidation sequence was performed at 0 °C, (-)-19-*epi*-arborisidine (-)-96 was obtained in 87% yield from compound **95** but epimerised to (-)-arborisidine (-)-89 under

basic conditions (Scheme 11). The authors speculated that 19-*epi*-arborisidine might be also an isolable natural product if the isolation process was not performed under basic conditions.

(+)-Arborescidine C **97** (Fig. 7) is a naturally occurring tetracyclic indole alkaloid of biological interest, with antibacterial, antinematode, antiviral and antidepressant activity.<sup>99</sup> It was isolated from *Pseudodistoma arborescens*, a marine tunicate, and from the sponge *Verongula rigida*. Due to its biological significance, many synthetic approaches have been explored.<sup>93,100–102</sup> (+)-Arborescidine B **98** is closely structurally related to (+)-arborescidine C **97**, and part of the brominated marine alkaloid family with a tetracyclic indole core (Fig. 7).

Hong and collaborators described the enantioselective synthesis of these natural compounds using the Pictet–Spengler reaction catalysed by asymmetric organocatalysts.<sup>103</sup> The best results were obtained for the acyl-Pictet–Spengler reaction with tryptamine **75** and aldehyde **99** using thiourea **100**, in diethyl



**Scheme 11** Synthesis of (-)-19-*epi*-arborisidine (-)-96 and (-)-arborisidine (-)-89. (a) i. TFA, paraformaldehyde, toluene/MeCN 3 : 1 and ii. PhIO, 0 °C, 87%. (b) Toluene/MeCN 3 : 1, 2 N aqueous KOH, rt, 57%.



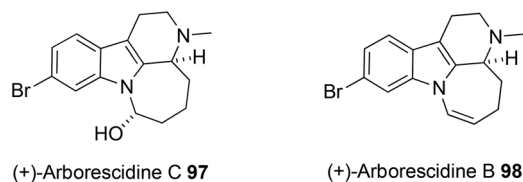


**Fig. 7** Structures of (+)-arborescicine C **97** and (+)-arborescicine B **98**.

ether at  $-60\text{ }^{\circ}\text{C}$  for 37 hours, affording product **101** in 74% yield and 95% ee (Scheme 12).

For the synthesis of desbromoarborescicine C **103** two approaches were tested.<sup>103</sup> The first strategy was based on the one-pot acyl-Pictet–Spengler reaction of tryptamine **75** with aldehyde **99**, catalysed by thiourea **100**, giving amide **101** in 63% yield and 93% ee followed by an amide reduction with  $\text{LiH}_2\text{NBH}_3$  to afford **102**. The reductive amination of **102** in the presence of formaldehyde and  $\text{NaBH}_3\text{CN}$ , followed by hydrolysis of the acetal and cyclisation afforded desbromoarborescicine C **103** in 97% ee (Scheme 12). Treatment of **103** with  $\text{MsCl}$  and  $\text{Et}_3\text{N}$  afforded desbromoarborescicine B **104** in very good yield (72%, Scheme 12). The other synthetic approach was based on the methylformyl-Pictet–Spengler reaction; however, the enantiomeric excess was lower (74% ee).<sup>103</sup>

The synthesis of (+)-arborescicine C **97** was accomplished using the one-pot thiourea **100** catalysed acyl-Pictet–Spengler reaction approach and compound **106** was obtained in 54% yield and 83% enantiomeric excess (Scheme 13). This amide was reduced to the corresponding amine **107** in 67% yield. The reductive amination of **107** followed by acetal hydrolysis and cyclisation gave (+)-arborescicine C **97** in 76% yield and

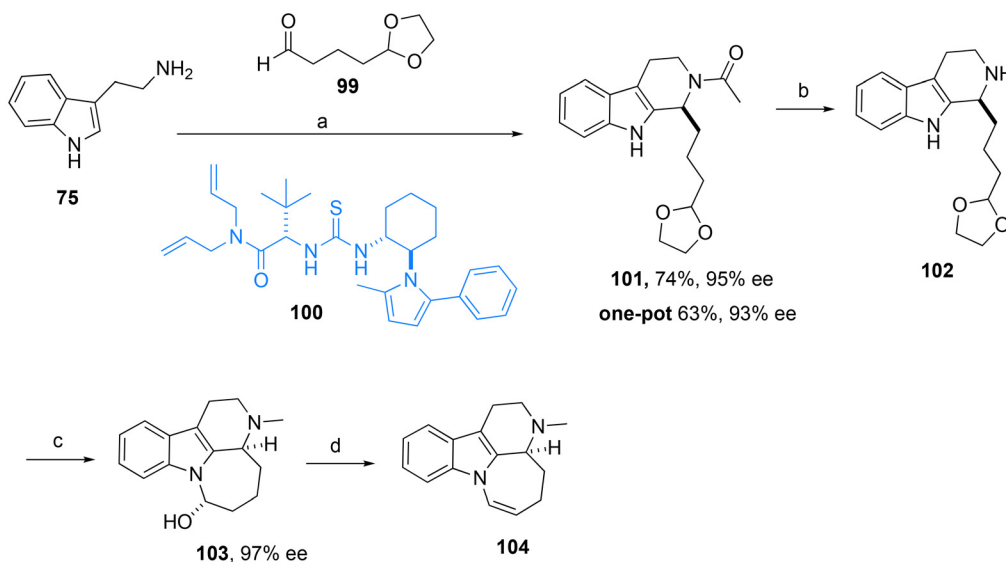
86% ee. Arborescicine B **98** was easily synthesised by dehydration of **97** (Scheme 13).

The asymmetric Pictet–Spengler reaction using a Jacobsen-type thiourea organocatalyst led to a highly enantioselective and efficient synthesis of (+)-arborescicine C and related tetracyclic indole alkaloids.<sup>103</sup>

This reaction type was once more used for the challenging enantioselective synthesis of another member of the large indole alkaloid, proving its wide applicability. Zhu *et al.* described the synthesis of (+)-alstratine A **108** (Scheme 14), a hexacyclic cage-like monoterpene indole alkaloid, *via* an organocatalytic enantioselective Pictet–Spengler reaction of  $\alpha$ -ketoesters.<sup>110</sup> (+)-Alstratine A is a structurally complex natural product isolated from members of the *Alstonia* genus (family Apocynaceae), which are known for their rich alkaloid content. (+)-Alstratine A **108** possesses a 1,1-disubstituted tetrahydro- $\beta$ -carboline (THBC) core, which is found in many bioactive natural products.<sup>104–109</sup>

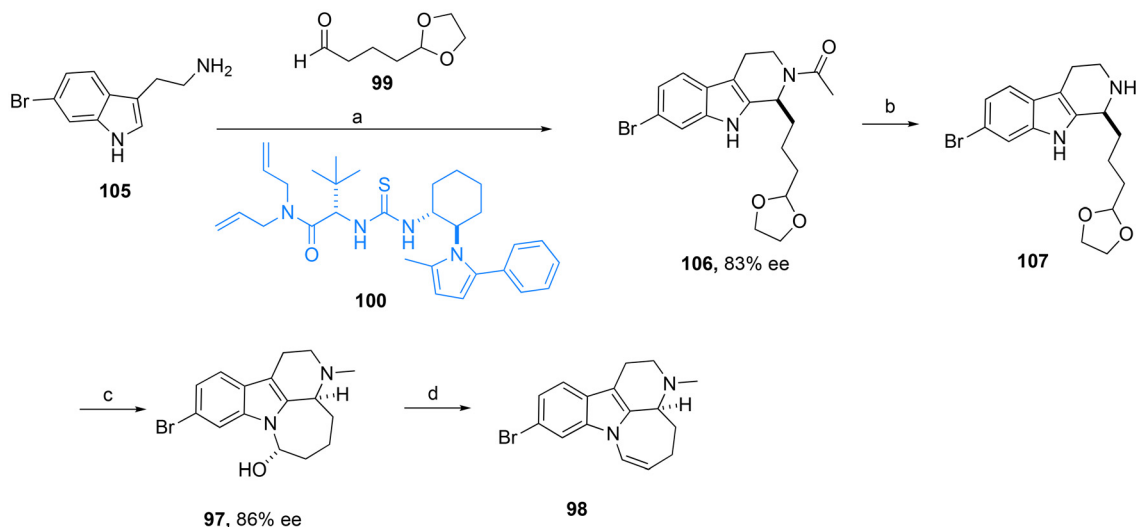
The authors developed a squaramide-catalysed asymmetric Pictet–Spengler reaction between tryptamines and methyl 2-oxoalkanoates, which afforded 1-alkyl-1-methoxycarbonyl tetrahydro- $\beta$ -carbolines (THBCs) with high yields and enantiomeric excess values. The reaction showed a wide application scope, tolerating various functional groups including heterocycles, ethers, esters, acetals, alkenes and azides.<sup>110</sup> High yields were obtained (63% to 95%) and the products presented high ee (79%–99%). This methodology was applied to synthesise (+)-alstratine A (Scheme 14).

The total synthesis was accomplished in seven steps with only four purifications of synthetic intermediates. Key steps in the synthesis included the enantioselective Pictet–Spengler reaction catalysed by squaramide **110**, giving the desired product **111** in 98% yield and 92% ee. The chemoselective

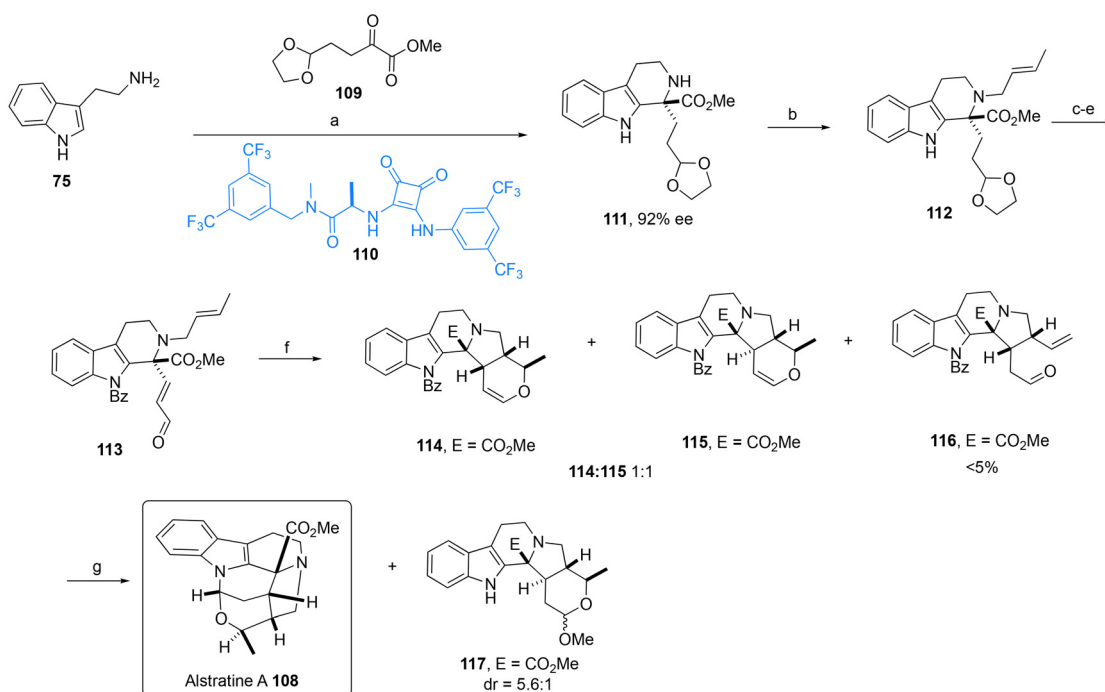


**Scheme 12** Synthesis of the cyclic indole system **104**. (a) i. **99**,  $\text{Na}_2\text{SO}_4$ ,  $\text{CH}_2\text{Cl}_2$ – $\text{Et}_2\text{O}$  (3 : 1), rt, 2 h and ii. **100**, 2,6-lutidine,  $\text{AcCl}$ ,  $\text{Et}_2\text{O}$ ,  $-78\text{ }^{\circ}\text{C}$  to  $-60\text{ }^{\circ}\text{C}$ , 37 h. (b)  $\text{LiH}_2\text{NBH}_3$ , THF,  $0\text{ }^{\circ}\text{C}$  to  $60\text{ }^{\circ}\text{C}$ , 4 h, 69%. (c) i.  $\text{NaBH}_3\text{CN}$ , 37% HCHO, MeOH,  $0\text{ }^{\circ}\text{C}$  to rt, 12 h and ii. aq. 2 N HCl, THF, 3 h, 72%. (d)  $\text{MsCl}$ ,  $\text{Et}_3\text{N}$ ,  $\text{CH}_2\text{Cl}_2$ , 2 h, 72%.





**Scheme 13** Synthesis of (+)-arborescidine B **98**. (a) i. **99**, Na<sub>2</sub>SO<sub>4</sub>, CH<sub>2</sub>Cl<sub>2</sub>:Et<sub>2</sub>O (3:1), rt, 2 h and ii. **100**, 2,6-lutidine, AcCl, Et<sub>2</sub>O–CH<sub>2</sub>Cl<sub>2</sub> (9:1), –78 °C to –60 °C, 26 h, 54%. (b) LiH<sub>2</sub>NBH<sub>3</sub>, THF, 0 °C to 60 °C, 4 h, 67%. (c) i. NaBH<sub>3</sub>CN, 37% HCHO, MeOH, 0 °C to rt, 12 h and ii. aq. 2 N HCl, THF, 3 h, 76%. (d) MsCl, Et<sub>3</sub>N, CH<sub>2</sub>Cl<sub>2</sub>, 2 h, 79%.



**Scheme 14** Synthesis of (+)-alstratine A **108**. (a) **110** (0.2 equiv.), salicylic acid, 5 Å MS, toluene (c 0.04 M), 0 °C, 3 days, 98%. (b) (*E*)-Crotyl bromide, K<sub>2</sub>CO<sub>3</sub>, MeCN, 50 °C, 91%. (c) PhCOCl, Et<sub>3</sub>N, DMAP, CH<sub>2</sub>Cl<sub>2</sub>, rt, 85%. (d) HCl 3 N/acetone (1:1), 0 °C to rt. (e) IBX, DMSO, 65 °C. (f) Mesitylene, reflux. (g) i. K<sub>2</sub>CO<sub>3</sub>, MeOH, rt, ii. HCl 6 N, rt: **108** obtained in 24% yield over 4 steps, **117** obtained in 22% yield over 4 steps.

*N*-crotylation afforded compound **112** in 91% yield (Scheme 14). *N*-Benzoylation, hydrolysis of the dioxolane and oxidation of the resulting aldehyde with IBX afforded the  $\alpha,\beta$ -unsaturated aldehyde **113**. A subsequent intramolecular hetero-Diels–Alder reaction afforded the two diastereomers **114** and **115** (1:1) and byproduct **116** (less than 5%). The Diels–Alder adducts **114** and **115** were treated with potassium

carbonate in methanol, followed by 6 N HCl, affording (+)-alstratine A **108** (24% overall yield in last 4 steps).<sup>110</sup>

The absolute configuration of the synthesised (+)-alstratine A was confirmed by X-ray diffraction analysis. An interesting insight from this work was the correction of a previously reported property of (+)-alstratine A. While the absolute configuration determined for (+)-alstratine A was correct, the



natural product is dextrorotatory, rather than levorotatory as initially reported in the isolation paper.<sup>104</sup> This highlights the importance of synthetic studies for confirming and sometimes correcting the reported properties of isolated natural products. Additionally, this work confirmed the potential of organocatalytic methods in the synthesis of complex natural products, offering an efficient and enantioselective approach to construct challenging molecular structures.

5,22-Dioxokopsane **118**, kopsinidine C **119** and demethoxycarbonylkopsin **120** (Fig. 8) are also indole alkaloids derived from plants of the Apocynaceae family, particularly from species within the genus *Kopsia*. *Kopsia* species are known for producing structurally complex monoterpene indole alkaloids, which have attracted attention due to their pharmacological properties.<sup>111,112</sup>

3,3-Disubstituted carbazolones are valuable building blocks for assembling *Aspidosperma* and *Kopsia* indole alkaloids.<sup>113–117</sup> Dawei Ma and collaborators described the use of asymmetric Michael addition of carbazolones to 2-chloroacrylonitrile, catalysed by a modified Takemoto thiourea catalyst.

A highly enantioselective method for synthesising the desired 3,3-disubstituted carbazolones was thus developed (Scheme 15).<sup>118</sup>

The catalyst structure, substrate scope and reaction conditions were evaluated.<sup>118</sup> Ma and collaborators systematically modified the Takemoto thiourea catalyst to improve its efficiency for the specific substrates in their study. They found that fine-tuning the amine part of the catalyst, particularly using an *N*-cyclopentyl-*N*-*n*-pentyl-amino-substituted thiourea, provided the best results in terms of yield and enantioselectivity. The *N*-*n*-pentyl group, a bulky group, afforded excellent yield and enantioselectivity (>95% yield and 95% ee) compared to thioureas with shorter *N*-alkyl substituents (methyl to *n*-butyl). However, replacing the cyclopentyl group in an amine with a cyclohexyl group led to a decrease in both yield and enantioselectivity (62% yield and 65% ee). The best organocatalyst was applied to various substituted carbazolones and related heterocycles, demonstrating a broad substrate scope with excellent yields and enantioselectivities.

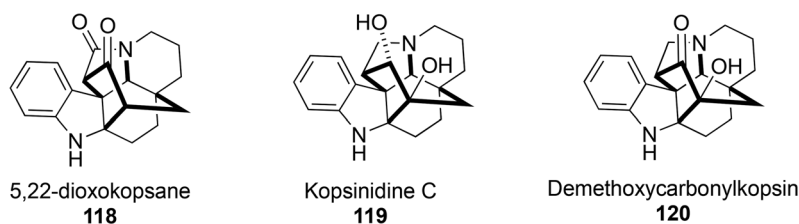
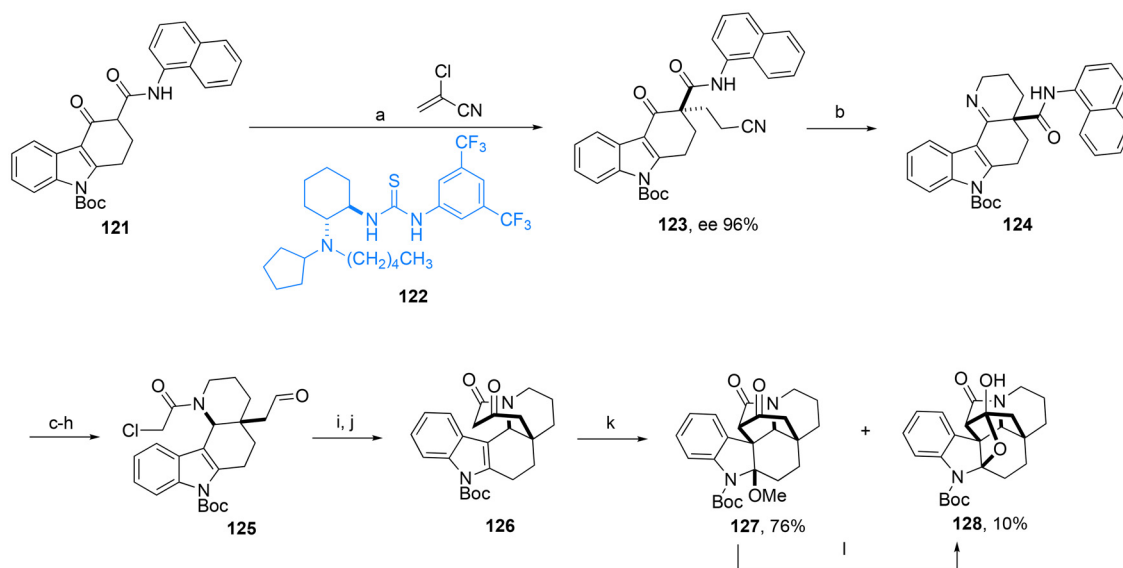
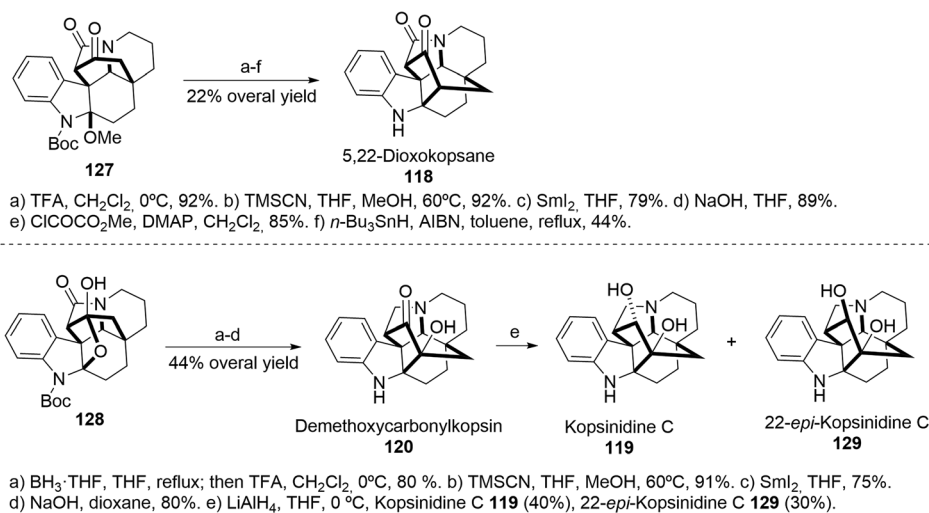


Fig. 8 Structures of 5,22-dioxokopsane **118**, kopsinidine C **119** and demethoxycarbonylkopsin **120**.



Scheme 15 Synthesis of intermediates **127** and **128**. (a) i. 10 mol% **122**, toluene,  $-10\text{ }^{\circ}\text{C}$  and ii. Zn, AcOH, THF, rt, >95%. (b) RANEY® Ni, H<sub>2</sub>, MeOH, 75%. (c) (Boc)<sub>2</sub>O, DMAP, THF, 94%. (d) DIBAL-H,  $-78\text{ }^{\circ}\text{C}$  to  $0\text{ }^{\circ}\text{C}$ , 65%. (e) Pd/C, H<sub>2</sub>, EtOAc, 82%. (f) SO<sub>3</sub>·Py, DMSO, Et<sub>3</sub>N, CH<sub>2</sub>Cl<sub>2</sub> 81%, 98% ee. (g) PPh<sub>3</sub><sup>+</sup>CH<sub>2</sub>OMeCl<sup>-</sup>, *t*-BuOK, THF,  $0\text{ }^{\circ}\text{C}$  to rt, 79%. (h) i. ClCH<sub>2</sub>COCl, aq. Na<sub>2</sub>CO<sub>3</sub>, THF and ii. 1 N HCl, 79%. (i) Sml<sub>2</sub>, THF. (j) Dess–Martin periodinane, NaHCO<sub>3</sub>, CH<sub>2</sub>Cl<sub>2</sub>,  $0\text{ }^{\circ}\text{C}$ , 53% over 2 steps. (k) Mn(OAc)<sub>3</sub>, H<sub>2</sub>O, Cu(OAc)<sub>2</sub>, MeOH, rt. (l) 1 N HCl, THF, 94%.





**Scheme 16** Synthesis of 5,22-dioxokopsane **118**, kopsinidine C **119**, demethoxycarbonylkopsin **120** and 22-*epi*-kopsinidine C **129**.

Ma *et al.* described the application of this method to the total syntheses of three *Kopsia* alkaloids: 5,22-dioxokopsane **118**, kopsinidine C **119** and demethoxycarbonylkopsin **120** (Schemes 15 and 16). The optimised Michael addition of  $\beta$ -ketoamide **121** to chloroacrylonitrile, catalysed by thiourea **122**, afforded **123** in excellent yield (>95%) and enantiomeric excess (96%). This reaction was successfully scaled up to 9 g, using 5 mol% of **122**. RANEY® nickel reductive cyclisation of **123** afforded tetracyclic imine **124** in 75% yield. A key step of the synthetic strategy involved the SmI<sub>2</sub>-mediated Reformatsky-type cyclisation of **125**, yielding an alcohol that was directly oxidised, using Dess–Martin periodinane, to afford  $\beta$ -ketoamide **126** in 53% yield (2 steps).

The synthetic route involved a Mn<sup>(III)</sup>-mediated oxidative cyclisation to create the caged ring system, giving two cyclisation products, **127** and **128**, in yields of 76% and 10%, respectively.  $\beta$ -Ketoamide **127** was transformed under acidic conditions into hemiacetal **128** in 94% yield (Scheme 15). These two compounds were important intermediates in the synthesis of the *Kopsia* alkaloids (Scheme 16).

These syntheses demonstrated the utility of the developed Michael addition method in complex alkaloid synthesis. This work presented several unique and interesting insights. First, it showcases the power of fine-tuning organocatalyst structures to achieve high efficiency and selectivity in challenging reactions. The success in modifying the Takemoto catalyst for this specific transformation may inspire further organocatalyst development. Second, the Mn<sup>(III)</sup>-mediated oxidative cyclisation provides a novel and reliable strategy for constructing the indole C3 quaternary stereocentre, a common structural feature in many indole alkaloids. Lastly, the research addresses a long-standing challenge in synthesising 3,3-disubstituted carbazolones, offering an alternative approach to the previously reported palladium-catalysed decarboxylative allylation method. This new method's high enantioselectivity and

efficiency, even on larger scales, make it a valuable tool for the synthesis of complex alkaloids and potentially other natural products.

## Conclusion

This review highlights the transformative impact of thiourea and squaramide organocatalysts in the asymmetric total synthesis of complex natural products. Several landmark achievements in the total synthesis of natural products using these catalysts were described. Notably, the enantioselective syntheses of *Aspidosperma* alkaloids such as (–)-minovincine, (–)-aspidofractinine and (+)-vincadifformine were accomplished through innovative cascade strategies and the use of bifunctional organocatalysts, demonstrating both scalability and exceptional stereochemical control.

The review also details the thiourea-catalysed sequential Michael addition that enabled the synthesis of Calycanthaceae alkaloids, including (–)-calycanthine, (+)-chimonanthine and (+)-folicanthine, with high yields and enantioselectivities, and the ability to access both enantiomers. A notable achievement was the highly enantioselective organocatalytic desymmetrisation that facilitated the efficient, multigram-scale synthesis of the marine alkaloid madangamine E, introducing multiple stereocentres with very high selectivity. Additionally, the successful application of thiourea catalysis in the synthesis of other architecturally complex natural products, such as caprazamycin A, was discussed.

In summary, all the works described in this review highlight the importance and versatility of thiourea- and squaramide-mediated organocatalysis to construct complex synthetic intermediates with high enantioselectivity and efficiency.



For synthetic chemists, the practical advantages of thiourea and squaramide catalysts, including ease of handling, broad substrate compatibility and tunability, make them indispensable tools for tackling the stereoselective synthesis of structurally challenging targets, with broad implications for both fundamental research and pharmaceutical innovation. Applications in cascade reactions, late-stage functionalisation and total synthesis of densely functionalised natural products will continue to drive the evolution of hydrogen-bond-mediated organocatalysis as a highly valuable strategy in advanced asymmetric synthesis.

## Future outlook

The field of organocatalysis, particularly using thiourea and squaramide catalysts, has immense potential for further innovation and impact. As demonstrated in this review, these catalysts have already enabled the highly selective and efficient synthesis of some structurally complex and biologically significant natural products.

The continued development of new catalyst architectures, especially those that combine the best features of thioureas, squaramides and other hydrogen-bonding motifs, will lead to even greater catalytic efficiency, broader substrate scope and improved stereocontrol. Advances in computational chemistry and mechanistic understanding will further inform the rational design of next-generation organocatalysts, allowing chemists to tailor catalysts for specific synthetic challenges and to predict and optimise reaction outcomes with increasing precision.

The application of organocatalysis to even more complex and diverse natural product targets is expected to expand. As new families of bioactive compounds are discovered, the mild, metal-free and highly selective nature of thiourea and squaramide catalysts will make them particularly valuable for constructing challenging molecular architectures and for the functionalisation of advanced intermediates. The integration of organocatalytic methods with other synthetic strategies, such as photoredox catalysis, biocatalysis and flow chemistry, also holds promise for multi-step syntheses and improving overall efficiency and sustainability.

The scalability and operational simplicity of organocatalytic processes position them as attractive tools for industrial applications, including pharmaceutical drug synthesis. Industry is favouring greener and more sustainable chemistry; thus the adoption of organocatalytic methodologies is likely to accelerate, especially for the synthesis of active pharmaceutical ingredients and complex drug candidates.

Finally, the ongoing exploration of new reactivity modes and activation strategies, such as cooperative catalysis, dual catalysis and the use of organocatalysts in tandem or cascade reactions, will allow chemists to achieve levels of complexity and efficiency in synthesis that were previously out of reach. The ability to construct multiple stereocentres in a single operation, or to achieve challenging transformations under exceptionally mild conditions, will remain a driving force for innovation.

In summary, the prospects for thiourea and squaramide organocatalysis remain highly promising. As the field continues to evolve, ongoing advances in catalyst design, mechanistic understanding and synthetic methodology are expected to further expand the scope, efficiency and selectivity of these catalytic systems to provide practical solutions to some of the most pressing challenges in natural product synthesis, drug discovery and sustainable chemistry.

## Conflicts of interest

There are no conflicts to declare.

## Data availability

No primary research results, software or code have been included and no new data were generated or analysed as part of this review.

## Acknowledgements

This work was supported by Fundação para a Ciência e Tecnologia (FCT) through a grant to M. R. (PD/BD/135494/2018) and (COVID/BD/152506/2022) and through MOSTMICRO-ITQB R&D Unit (UIDB/04612/2020, UIDP/04612/2020) and LS4FUTURE Associated Laboratory (LA/P/0087/2020).

## References

- 1 D. W. C. MacMillan, *Nature*, 2008, **455**, 304–308.
- 2 M. R. Ventura, *Mini. Rev. Org. Chem.*, 2014, **11**, 154–163.
- 3 I. Jain and P. Malik, *Eur. Polym. J.*, 2020, **133**, 109791.
- 4 J. Gomez-Vega, A. Vasquez-Cornejo, O. Juárez-Sánchez, D. O. Corona-Martínez, A. Ochoa-Terán, K. A. López-Gastelum, R. R. Sotelo-Mundo, H. Santacruz-Ortega, J. C. Gálvez-Ruiz, R. Pérez-González and K. O. Lara, *ACS Omega*, 2024, **9**, 4412–4422.
- 5 E. Fan, S. A. Van Arman, S. Kincaid and A. D. Hamilton, *J. Am. Chem. Soc.*, 1993, **115**, 369–370.
- 6 V. Kumar, *Bull. Chem. Soc. Jpn.*, 2021, **94**, 309–326.
- 7 V. K. Bhardwaj, S. Sharma, N. Singh, M. S. Hundal and G. Hundal, *Supramol. Chem.*, 2011, **23**, 790–800.
- 8 P. Das, P. Mahato, A. Ghosh, A. K. Mandal, T. Banerjee, S. Saha and A. Das, *J. Chem. Sci.*, 2011, **123**, 175–186.
- 9 P. R. Schreiner and A. Wittkopp, *Org. Lett.*, 2002, **4**, 217–220.
- 10 A. Wittkopp and P. R. Schreiner, *Chem. – Eur. J.*, 2003, **9**, 407–414.
- 11 M. S. Sigman and E. N. Jacobsen, *J. Am. Chem. Soc.*, 1998, **120**, 4901–4902.
- 12 M. S. Sigman, P. Vachal and E. N. Jacobsen, *Angew. Chem., Int. Ed.*, 2000, **39**, 1279–1281.



- 13 P. Vachal and E. N. Jacobsen, *J. Am. Chem. Soc.*, 2002, **124**, 10012–10014.
- 14 A. G. Wenzel and E. N. Jacobsen, *J. Am. Chem. Soc.*, 2002, **124**, 12964–12965.
- 15 E. J. Corey and M. J. Grogan, *Org. Lett.*, 1999, **1**, 157–160.
- 16 T. Okino, Y. Hoashi and Y. Takemoto, *J. Am. Chem. Soc.*, 2003, **125**, 12672–12673.
- 17 T. Okino, Y. Hoashi, T. Furukawa, X. Xu and Y. Takemoto, *J. Am. Chem. Soc.*, 2005, **127**, 119–125.
- 18 C. Cao, M. Ye, X. Sun and Y. Tang, *Org. Lett.*, 2006, **8**, 2901–2904.
- 19 H. Miyabe and Y. Takemoto, *Bull. Chem. Soc. Jpn.*, 2008, **81**, 785–795.
- 20 X. J. Zhang, S. P. Liu, J. H. Lao, G. J. Du, M. Yan and A. S. C. Chan, *Tetrahedron: Asymmetry*, 2009, **20**, 1451–1458.
- 21 L. J. Yan, Q. Z. Liu and X. L. Wang, *Chin. Chem. Lett.*, 2009, **20**, 310–313.
- 22 Y. Takemoto, *Chem. Pharm. Bull.*, 2010, **58**, 593–601.
- 23 S. Konda and J. C. G. Zhao, *Tetrahedron Lett.*, 2014, **55**, 5216–5218.
- 24 R. S. Malkar, A. L. Jadhav and G. D. Yadav, *Mol. Catal.*, 2020, **485**, 110814.
- 25 M. Rénio, D. Murtinho and M. R. Ventura, *Chirality*, 2022, **34**, 782–795.
- 26 N. Wang, Z. Wu, J. Wang, N. Ullah and Y. Lu, *Chem. Soc. Rev.*, 2021, **50**, 9766–9793.
- 27 T. Parvin, R. Yadav and L. H. Choudhury, *Org. Biomol. Chem.*, 2020, **18**, 5513–5532.
- 28 P. S. Bhadury and J. Pang, *Curr. Org. Chem.*, 2021, **26**, 2–5.
- 29 E. Sansinenea and A. Ortiz, *Curr. Org. Synth.*, 2021, **19**, 148–165.
- 30 A. Biswas, H. Mondal and M. S. Maji, *J. Heterocycl. Chem.*, 2020, **57**, 3818–3844.
- 31 R. Parella, S. Jakkampudi and J. C. G. Zhao, *ChemistrySelect*, 2021, **6**, 2252–2280.
- 32 F. Vetica, P. Chauhan, S. Dochain and D. Enders, *Chem. Soc. Rev.*, 2017, **46**, 1661–1674.
- 33 J. Kaur, S. Kaur and K. Kaur, *ChemistrySelect*, 2024, **9**, e202305181.
- 34 B. Ullah, N. K. Gupta, Q. Ke, N. Ullah, X. Cai and D. Liu, *Catalysts*, 2022, **12**, 1149.
- 35 P. Sharma, R. Gupta and R. K. Bansal, *Beilstein J. Org. Chem.*, 2021, **17**, 2585–2610.
- 36 I. Bagheri, L. Mohammadi, V. Zadsirjan and M. M. Heravi, *ChemistrySelect*, 2021, **6**, 1008–1066.
- 37 H. Joshi and V. K. Singh, *Asian J. Org. Chem.*, 2022, **11**, e202100053.
- 38 Z. W. Zhang, S. W. Liu, H. P. Huang, Y. H. Xie, R. C. Huang, Y. Q. Deng and N. Lin, *RSC Adv.*, 2023, **13**, 31047–31058.
- 39 V. L. de Almeida, C. G. Silva, A. F. Silva, P. R. V. Campana, K. Foubert, J. C. D. Lopes and L. Pieters, *J. Ethnopharmacol.*, 2019, **231**, 125–140.
- 40 S. Varga, P. Angyal, G. Martin, O. Egyed, T. Holczbauer and T. Soós, *Angew. Chem., Int. Ed.*, 2020, **59**, 13547–13551.
- 41 J. M. Saya, E. Ruijter and R. V. A. Orru, *Chem. – Eur. J.*, 2019, 8916.
- 42 B. N. Laforteza, M. Pickworth and D. W. C. MacMillan, *Angew. Chem., Int. Ed.*, 2013, **52**, 11269–11272.
- 43 T. Morikawa, S. Harada and A. Nishida, *J. Org. Chem.*, 2015, **80**, 8859–8867.
- 44 B. Berkes, K. Ozsváth, L. Molnár, T. Gáti, T. Holczbauer, G. Kardos and T. Soós, *Chem. – Eur. J.*, 2016, **22**, 18101.
- 45 C. Djerassi, H. Budzikiewicz, J. M. Wilson, J. Gosset, J. Le Men and M. M. Janot, *Tetrahedron Lett.*, 1962, **3**, 235–239.
- 46 L. Pan, C. W. Zheng, G. S. Fang, H. R. Hong, J. Liu, L. H. Yu and G. Zhao, *Chem. – Eur. J.*, 2019, **25**, 6306.
- 47 M. G. Hollingshead, M. C. Alley, R. F. Camalier, B. J. Abbott, J. G. Mayo, L. Malspeis and M. R. Grever, *Life Sci.*, 1995, **57**, 131–141.
- 48 S. B. Jones, B. Simmons, A. Mastracchio and D. W. C. MacMillan, *Nature*, 2011, **475**, 183–188.
- 49 M. A. Toczko and C. H. Heathcock, *J. Org. Chem.*, 2000, **65**, 4792–4801.
- 50 A. Khatua, D. Jana, M. Nandy, P. Shyamal and A. Bisai, *J. Org. Chem.*, 2024, **89**, 4792–4801.
- 51 R. H. F. Manske, *Alkaloids Chem. Physiol.*, 1965, **8**, 581–589.
- 52 M. Kitajima, I. Mori, K. Arai, N. Kogure and H. Takayama, *Tetrahedron Lett.*, 2006, **47**, 3199–3202.
- 53 J. A. May and B. Stoltz, *Tetrahedron*, 2006, **62**, 5262–5271.
- 54 X. Shen, T. Peng, Y. Zhou, Y. Xi, J. Zhao, X. Yang and H. Zhang, *Chin. J. Org. Chem.*, 2019, 2685–2704.
- 55 L. E. Overman, D. V. Paone and B. A. Stearns, *J. Am. Chem. Soc.*, 1999, **121**, 7702–7703.
- 56 L. E. Overman, J. F. Larrow, B. A. Stearns and J. M. Vance, *Angew. Chem., Int. Ed.*, 2000, **39**, 213–215.
- 57 M. Movassaghi and M. A. Schmidt, *Angew. Chem., Int. Ed.*, 2007, **46**, 3725–3728.
- 58 J. B. Xu and K. J. Cheng, *Molecules*, 2015, **20**, 6715–6738.
- 59 F. Kong, R. J. Andersen and T. M. Allen, *J. Am. Chem. Soc.*, 1994, **116**, 6007–6008.
- 60 F. Kong, E. I. Graziani and R. J. Andersen, *J. Nat. Prod.*, 1998, **61**, 267–271.
- 61 M. Amat, M. Pérez, R. Ballette, S. Proto and J. Bosch, *Alkaloids Chem. Biol.*, 2015, **74**, 159–199.
- 62 K. Miura, S. Kawano, T. Suto, T. Sato, N. Chida and S. Simizu, *Bioorg. Med. Chem.*, 2021, **34**, 116041.
- 63 R. G. S. Berlinck, in *Bioactive Heterocycles IV*, 2007, pp. 211–238.
- 64 B. Cheng and J. Reyes, *Nat. Prod. Rep.*, 2020, **37**, 322–337.
- 65 R. Ballette, M. Pérez, S. Proto, M. Amat and J. Bosch, *Angew. Chem., Int. Ed.*, 2014, **53**, 6202–6205.
- 66 C. Are, M. Pérez, J. Bosch and M. Amat, *Chem. Commun.*, 2019, **55**, 7207–7210.
- 67 T. Suto, Y. Yanagita, Y. Nagashima, S. Takikawa, Y. Kurosu, N. Matsuo, T. Sato and N. Chida, *J. Am. Chem. Soc.*, 2017, **139**, 2952–2955.
- 68 S. Shiomi, B. D. A. Shennan, K. Yamazaki, Á. L. Fuentes De Arriba, D. Vasu, T. A. Hamlin and D. J. Dixon, *J. Am. Chem. Soc.*, 2022, **144**, 1407–1415.



- 69 H. Nakamura, C. Tsukano, T. Yoshida, M. Yasui, S. Yokouchi, Y. Kobayashi, M. Igarashi and Y. Takemoto, *J. Am. Chem. Soc.*, 2019, **141**, 8527–8540.
- 70 M. Igarashi, N. Nakagawa, N. Doi, S. Hattori, H. Naganawa and M. Hamada, *J. Antibiot.*, 2003, **56**, 580–583.
- 71 M. Igarashi, Y. Takahashi, T. Shitara, H. Nakamura, H. Naganawa, T. Miyake and Y. Akamatsu, *J. Antibiot.*, 2005, **58**, 327–337.
- 72 G. W. Gribble, *Indole Ring Synthesis: From Natural Products to Drug Discovery*, 2016.
- 73 D. Shan, Y. Gao and Y. Jia, *Angew. Chem., Int. Ed.*, 2013, **52**, 4902–4905.
- 74 M. L. Bannasar, B. Vidal, B. A. Sufi and J. Bosch, *Chem. Commun.*, 1998, 2639–2640.
- 75 S. Zhao and R. B. Andrade, *J. Am. Chem. Soc.*, 2013, **135**, 13334–13337.
- 76 O. Wagnières, Z. Xu, Q. Wang and J. Zhu, *J. Am. Chem. Soc.*, 2014, **136**, 15102–15108.
- 77 B. Herlé, M. J. Wanner, J. H. Van Maarseveen and H. Hiemstra, *J. Org. Chem.*, 2011, **76**, 8907–8912.
- 78 L. A. Sharp and S. Z. Zard, *Org. Lett.*, 2006, **8**, 831–834.
- 79 M. J. Wanner, R. N. A. Boots, B. Eradus, R. De Gelder, J. H. Van Maarseveen and H. Hiemstra, *Org. Lett.*, 2009, **11**, 2579–2581.
- 80 D. Enders, A. Greb, K. Deckers, P. Selig and C. Merckens, *Chem. – Eur. J.*, 2012, **18**, 10226–10229.
- 81 K. B. Wang, Y. T. Di, Y. Bao, C. M. Yuan, G. Chen, D. H. Li, J. Bai, H. P. He, X. J. Hao, Y. H. Pei, Y. K. Jing, Z. L. Li and H. M. Hua, *Org. Lett.*, 2014, **16**, 3398–3401.
- 82 R. Andres, Q. Wang and J. Zhu, *J. Am. Chem. Soc.*, 2020, **142**, 14276–14285.
- 83 C. Piemontesi, Q. Wang and J. Zhu, *J. Am. Chem. Soc.*, 2016, **138**, 11148–11151.
- 84 D. Huang, F. Xu, X. Lin and Y. Wang, *Chem. – Eur. J.*, 2012, **18**, 3148–3152.
- 85 H. Schönherr and J. L. Leighton, *Org. Lett.*, 2012, **14**, 2610–2613.
- 86 C. A. Holloway, M. E. Muratore, R. L. Storer and D. J. Dixon, *Org. Lett.*, 2010, **12**, 4720–4723.
- 87 J. J. Badillo, A. Silva-García, B. H. Shupe, J. C. Fettingler and A. K. Franz, *Tetrahedron Lett.*, 2011, **52**, 5550–5553.
- 88 M. S. Taylor and E. N. Jacobsen, *J. Am. Chem. Soc.*, 2004, **126**, 13404–13405.
- 89 I. T. Raheem, P. S. Thiara, E. A. Peterson and E. N. Jacobsen, *J. Am. Chem. Soc.*, 2007, **129**, 13404–13405.
- 90 R. S. Klausen and E. N. Jacobsen, *Org. Lett.*, 2009, **11**, 887–890.
- 91 N. Mittal, D. X. Sun and D. Seidel, *Org. Lett.*, 2014, **16**, 1012–1015.
- 92 S. P. Wong, C. Y. Gan, K. H. Lim, K. N. Ting, Y. Y. Low and T. S. Kam, *Org. Lett.*, 2015, **17**, 3628–3631.
- 93 Z. Zhou, A. X. Gao and S. A. Snyder, *J. Am. Chem. Soc.*, 2019, **141**, 7715–7720.
- 94 P. Gan, J. Pitzen, P. Qu and S. A. Snyder, *J. Am. Chem. Soc.*, 2018, **140**, 919–925.
- 95 Z. Zhang, S. Xie, B. Cheng, H. Zhai and Y. Li, *J. Am. Chem. Soc.*, 2019, **141**, 7147–7154.
- 96 Z. Chen, T. Xiao, H. Song and Y. Qin, *Chin. J. Org. Chem.*, 2018, **38**, 2427–2434.
- 97 R. S. Klausen, C. R. Kennedy, A. M. Hyde and E. N. Jacobsen, *J. Am. Chem. Soc.*, 2017, **139**, 12299–12309.
- 98 S. M. Banik, A. Levina, A. M. Hyde and E. N. Jacobsen, *Science*, 2017, **358**, 6364.
- 99 S. P. Wong, K. W. Chong, K. H. Lim, S. H. Lim, Y. Y. Low and T. S. Kam, *Org. Lett.*, 2016, **18**, 1618–1621.
- 100 F. Y. Wang and L. Jiao, *Angew. Chem., Int. Ed.*, 2021, **60**, 12732–12736.
- 101 F. G. Erick and M. Carreira, *Synfacts*, 2020, **16**, 1143.
- 102 Z. Zhou, A. X. Gao and S. A. Snyder, *J. Am. Chem. Soc.*, 2019, **141**, 7715–7720.
- 103 V. M. Sheth, B. C. Hong and G. H. Lee, *Org. Biomol. Chem.*, 2017, **15**, 3408–3412.
- 104 J. Xie, X. Zou, C. Sang, M. Song, Q. Chen and J. Zhang, *Tetrahedron Lett.*, 2021, **75**, 153180.
- 105 W. T. Zhu, Q. Zhao, Z. Q. Huo, X. J. Hao, M. Yang and Y. Zhang, *Tetrahedron Lett.*, 2020, **61**, 152400.
- 106 C. E. Nge, C. Y. Gan, Y. Y. Low, N. F. Thomas and T. S. Kam, *Org. Lett.*, 2013, **15**, 4774–4777.
- 107 C. F. Ding, H. X. Ma, J. Yang, X. J. Qin, G. S. S. Njateng, H. F. Yu, X. Wei, Y. P. Liu, W. Y. Huang, Z. F. Yang, X. H. Wang and X. D. Luo, *Org. Lett.*, 2018, **20**, 2702–2706.
- 108 M. Rottmann, C. McNamara, B. K. S. Yeung, M. C. S. Lee, B. Zou, B. Russell, P. Seitz, D. M. Plouffe, N. V. Dharia, J. Tan, S. B. Cohen, K. R. Spencer, G. E. González-Páez, S. B. Lakshminarayana, A. Goh, R. Suwanarusk, T. Jegla, E. K. Schmitt, H. P. Beck, R. Brun, F. Nosten, L. Renia, V. Dartois, T. H. Keller, D. A. Fidock, E. A. Winzeler and T. T. Diagana, *Science*, 2010, **329**, 5996.
- 109 D. Fokas, L. Yu and C. M. Baldino, *Mol. Divers.*, 2005, **9**, 81–89.
- 110 R. Andres, F. Sun, Q. Wang and J. Zhu, *Angew. Chem., Int. Ed.*, 2023, **62**, e202213831.
- 111 Q. Jin, Y. L. Zhao, Y. P. Liu, R. S. Zhang, P. F. Zhu, L. Q. Zhao, X. J. Qin and X. D. Luo, *J. Ethnopharmacol.*, 2022, **285**, 114848.
- 112 S. Sudhir, R. D. Budhiraja, G. P. Miglani, B. Arora, L. C. Gupta and K. N. Garg, *Planta Med.*, 1986, 61–63.
- 113 J. d'Angelo and D. Desmaele, *Tetrahedron Lett.*, 1990, **31**, 879–882.
- 114 P. Jing, Z. Yang, C. Zhao, H. Zheng, B. Fang, X. Xie and X. She, *Chem. – Eur. J.*, 2012, **18**, 5782–5785.
- 115 C. J. Gartshore and D. W. Lupton, *Aust. J. Chem.*, 2013, **66**, 882–890.
- 116 L. Leng, X. Zhou, Q. Liao, F. Wang, H. Song, D. Zhang, X. Y. Liu and Y. Qin, *Angew. Chem., Int. Ed.*, 2017, **56**, 3703–3707.
- 117 C. J. Gartshore and D. W. Lupton, *Angew. Chem.*, 2013, **125**, 4113–4116.
- 118 D. Ni, Y. Wei and D. Ma, *Angew. Chem., Int. Ed.*, 2018, **57**, 10207–10211.

